

Identification of Random Material Properties using a Mixed Deterministic-Probabilistic Method¹

E. Dascotte

Dynamic Design Solutions N.V.
Interleuvenlaan 64, B-3001, Leuven, Belgium
E-mail: eddy.dascotte@dds.be

Abstract

To successfully make the move to digital prototyping, and thereby reduce the number of physical prototypes, predictions of product performance should be provided with a measure of confidence and validated against experimental data. Current model validation and updating practice, however, is based only on nominal values for input parameters and average test results. Recent advances in computing now make it feasible to incorporate scatter on input and output parameters as a logical extension to model validation and updating tools. Propagation of uncertainty throughout the structure can be studied, and realistic targets for model updating are set. Although some sources of scatter on input parameters can be directly observed and quantified, others may not. A mixed deterministic-probabilistic method is presented to extend identification of nominal values with identification of combined scatter on input parameters using statistical information obtained from repeated vibration tests. This method is demonstrated on the identification of elastic modulus of material samples.

1 Introduction

Uncertainty in numerical simulation results manifests itself in two main classes: physical uncertainty and numerical uncertainty.

There exist four main levels at which physical uncertainty, or scatter, becomes visible, namely

- **Boundary and initial conditions** - impact velocity, impact angle, mass of vehicle, characteristics of barriers, etc.
- **Material properties** - yield stress, strain-rate parameters, density, local imperfections, etc
- **Geometry** - shape, thickness, manufacturing and assembly tolerances, etc.
- **Loads** - earthquakes, wind gusts, sea waves, blasts, shocks, impacts, etc.

Uncertainty is further increased because many of these properties may vary substantially with temperature, frequency, or load level. Information on these forms of scatter can be obtained by measurement. A sufficient large number of samples need to be evaluated to distinguish the natural and intrinsic scatter from the (often high) scatter that may be attributed to a small number of statistical samples.

Probability distribution functions and their associated properties can be obtained from statistical analysis of the test data. For example, the elastic modulus of isotropic material can be described using a normal (Gaussian) distribution that is characterized by a mean value and standard deviation.

The following types of numerical uncertainty can be identified:

¹ Revised version of the paper presented at the ISMA 2004 conference held in Leuven, Belgium, Sep. 20-22, 2004.

- **Conceptual modeling uncertainty** - lack of data on the physical process involved, lack of system knowledge.
- **Mathematical modeling uncertainty** - accuracy of the mathematical model validity.
- **Discretization error uncertainties** – the choice of element types, mesh density, level of geometrical detail.
- **Numerical solution uncertainty** - rounding-off, convergence tolerances, integration step.
- **Human mistakes** - programming errors in the code or wrong utilization of the software, mistakes in data or units.

These types of scatter may or may not exist regardless of the physics involved. An example of the exhibit of numerical uncertainty is the different results that may be obtained by two finite element codes, using the same finite element model. Indeed changing solver, computing platform, or element formulation can be possible causes of significant differences.

It is clear that uncertainty also exists in testing. Possible causes of physical uncertainty are related to:

- **Test definition** – fixture, mounting procedure, excitation method, transducer location, sensor weight, dynamic loading.
- **Instrumentation** – calibration, distortions, cabling noise.
- **Data acquisition** – digital signal processing, measurement and filtering error.

Techniques like experimental modal analysis are also subject to numerical uncertainty in the mathematical models that are used for modal parameter estimation.

Making a complete inventory of all uncertainties in simulation and test is a challenging task. Moreover, not all uncertainties can be described in terms of statistical quantities and should rather be defined using minimum and maximum intervals. Examples of such uncertainties are the discretization error uncertainty and numerical solution uncertainty. Other uncertainty like human mistakes is rather incidental and should be detected and corrected as part of a continuous analysis quality assurance process.

2 Description of Procedure

The elastic material properties can be derived from the vibration behavior of test samples. For simple beam-like geometries using homogeneous isotropic material, the vibration behavior of the test specimen can be described by analytical formulas based on beam theory. Various methods based on these formulas exist, and have proven to produce repeatable and accurate results.

The finite element technique allows the modeling of the vibration behavior of test samples with an arbitrary shape combined with the use of more complex material models. In [1], an inverse method is used to identify the properties of orthotropic plates, by comparing calculated resonance frequencies of a finite element model of the test plate with experimentally measured frequencies. Recent work has extended this inverse method to identify the elastic properties of the individual layers of layered materials [2].

Figure 1 presents the general flowchart of the inverse method to identify elastic material properties. Initial values for the elastic material properties are estimated and introduced into the FE model of the test plate in order to compute the numerical resonance frequencies and frequency sensitivities of first global modes.

Improved material properties can be obtained from the differences between the experimental and numerical frequencies and frequency sensitivities by solving the following least-squares problem:

$$\{R_e\} = \{R_a\} + [S] (\{P_u\} - \{P_o\}) \quad (1)$$

Where:

$\{R_e\}$ Vector containing the reference system responses (experimental data).

$\{R_a\}$ Vector containing the predicted system responses for a given state $\{P_o\}$ of the parameter values.

$\{P_u\}$ Vector containing the updated parameter values (material properties).

$[S]$ Sensitivity matrix.

If the corrections of the material properties resulting from (1) are larger than the desired precision, the improved material properties are introduced into the FE-model and a new iteration is started, otherwise the updating routine is completed. If the frequencies of the FE-model of the last iteration match the experimental frequencies, the material properties of the test plate have been identified since they correspond with the material properties of the FE-model.

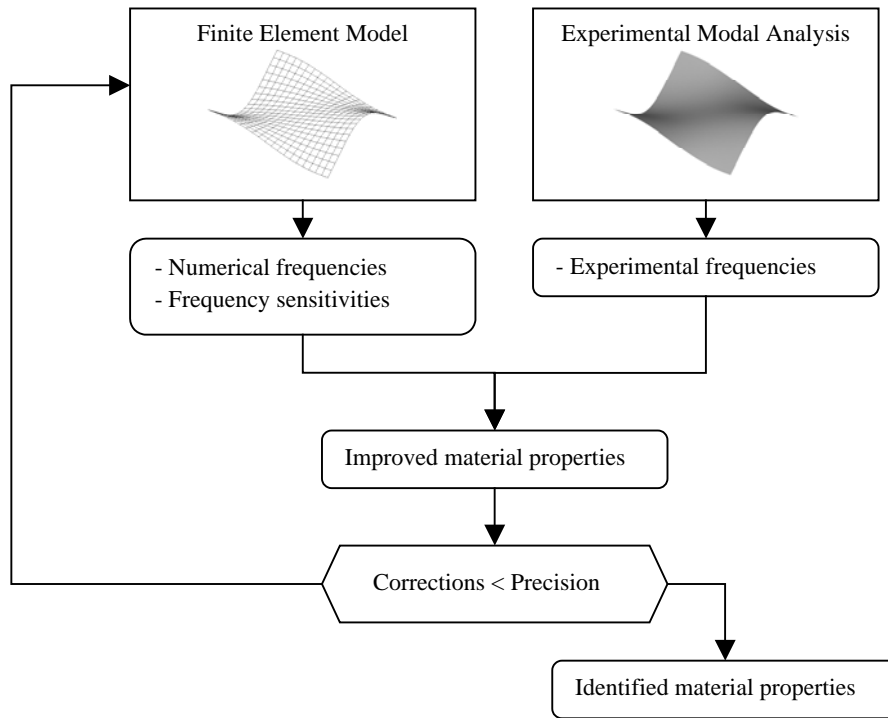


Figure 1: Flowchart of the inverse method for material identification.

In a real world, the uncertainties in model input parameters (e.g. material properties) and test data should be accounted for in a probabilistic updating method [3-4]. A mixed deterministic-probabilistic procedure, however, can be used as an intermediate step before the advent of entirely probabilistic procedures. In such an approach an initial updating of model input parameters is followed by a probabilistic analysis to estimate the random properties of the input parameter from the experimentally observed scatter on the responses values (resonance frequencies). This methodology is available in dedicated software [5].

3 Example Case

3.1 Test Data

The test sample is a rectangular aluminum beam. Table 1 presents the geometry and mass properties of this sample.

Length	76.190 mm
Width	6.436 mm
Thickness	6.366 mm
Mass	8.4386 gram

Table 1: The properties of the test sample.

Both the fundamental flexural frequency and torsion frequency were measured 100 times. The sample was excited by means of a miniature loudspeaker and the vibration signal was measured with a laser vibrometer [6].

Between each measurement the sample was removed from the test setup. In this way the spreading on the frequency also takes the variability of the sample position on the supporting wires into account.

The average flexural frequency was situated at 5536.25 Hz, and was measured with a sample frequency of 20 kHz. The average torsion frequency was situated at 19894.45 Hz and was measured with a sample frequency of 50 kHz. The excitation signal was a swept sine signal in the range [$f_{res}-500$ Hz, $f_{res}+500$ Hz]. The considered flexural frequency is associated with the vibration mode that causes a bending deformation in the width-direction, i.e. the considered flexural frequency is the higher of the two fundamental flexural frequencies. Additional statistical information reflecting the physical uncertainty on these tests is provided in table 2. Scatter is defined as the standard deviation divided by the mean value.

Mode	Mean (Hz)	St Dev (Hz)	Min (Hz)	Max (Hz)	Scatter (%)
Bending	5.5362E+3	2.6900E+0	5.5277E+3	5.5437E+3	0.0486
Torsion	1.9894E+4	3.1650E+1	1.9770E+4	1.9965E+4	0.1591

Table 2: Statistical properties of test data (100 samples).

The test results show very low scatter on both frequencies with the scatter on the torsional frequency three times larger than on the bending frequency. Figure 3 shows the scatter plot for all test data pairs. The figure shows that there is only a weak relationship between bending and torsional frequency. This indicates that there are two independent variables that govern these responses.

Histograms of the test data are shown in figures 4 and 5. The superposed continuous lines show the corresponding normal distribution with the same mean and standard deviation. It shows that the bending frequency measurements do not correspond to a normal distribution. The kurtosis (sharpness) of the observed distribution is much higher than that of a normal distribution. The observed distribution for the torsional frequency is closer to a normal distribution although she is not symmetric.

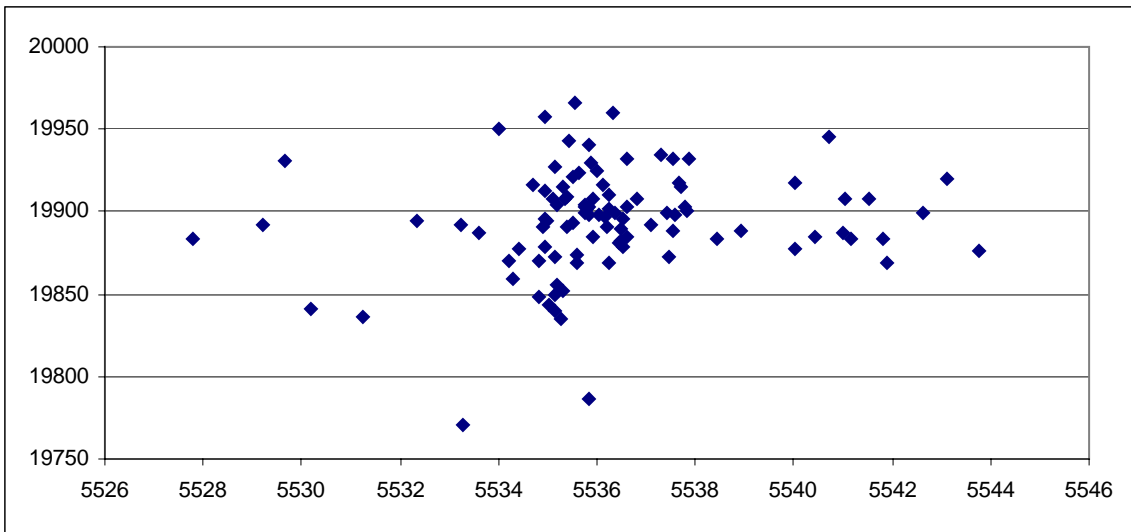


Figure 3: Scatter plot between tested bending (X-axis) and torsional (Y-axis) resonance frequencies.

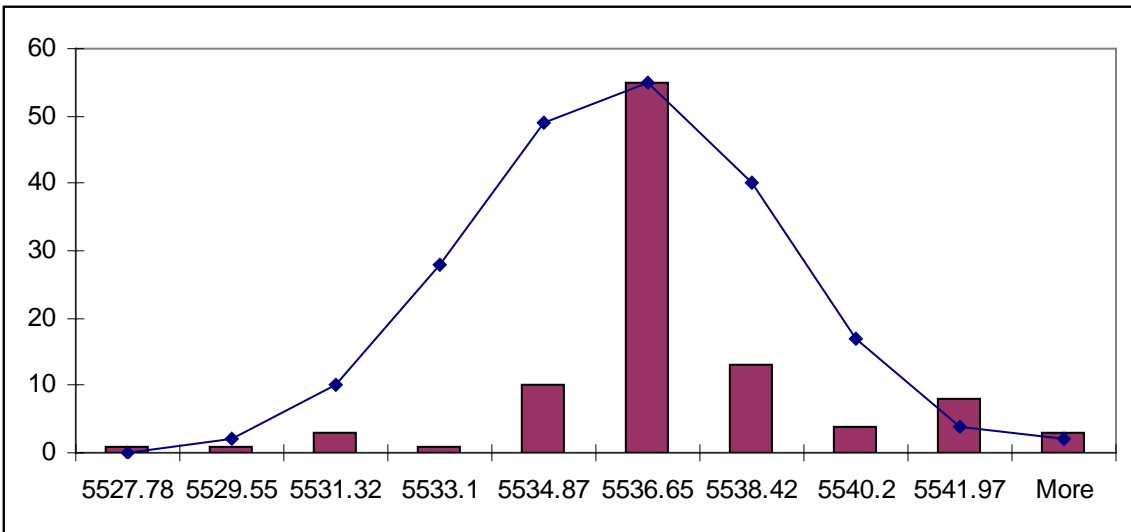


Figure 4: Histogram for bending resonance frequency.

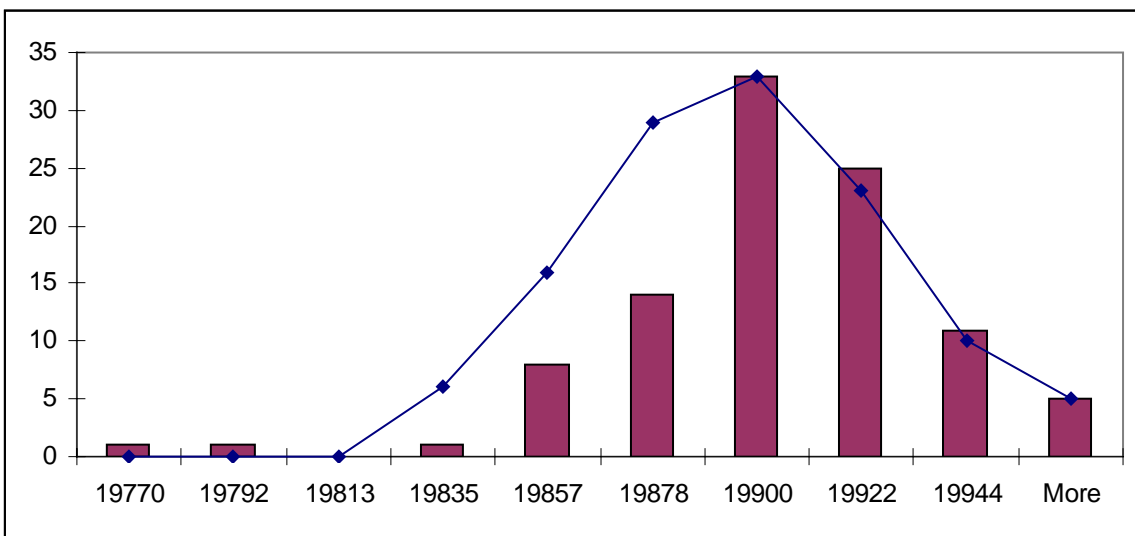


Figure 5: Histogram for torsional resonance frequency.

3.2 Finite Element Analysis

A finite element model using 20 general 3D beam elements was used to simulate the bending and torsional modes of the test sample. The starting value for the material properties were set to Young's modulus of 60 GPA, mass density of 2703 kg/m³ and Poisson ratio of 0.3. The beam cross sectional properties are derived from the measured dimension (see table 1), with shear section area factor 0.8333 which is valid for rectangular sections and torsional moment of inertia based on a handbook value. Note that several approximations for the torsional moment of inertia of a rectangular section are available in handbooks and selecting one therefore introduces uncertainty in the model.

A lumped mass formulation is used to compute the first 10 modes using the FEMtools solver. The results are shown in table 3. Because the section is not a perfect square, computed in-plane and out-of-plane modes appear in pairs but at slightly different frequencies.

Only the second and fifth modes are relevant in this analysis because they correspond with the measured values. Comparison with the mean measured values shows that these predictions are underestimated which can be explained by the low starting value for Young's modulus.

<u>Mode Nr.</u>	<u>Init. Frequency (Hz)</u>	<u>Test Frequency (Hz)</u>	<u>Relative Diff. (%)</u>
1	5212.76		
2	5268.82	5536.25	-4.83%
3	13886.63		
4	14027.44		
5	17594.87	19894.45	-11.56%
6	25959.53		
7	26201.04		
8	30885.61		
9	35081.27		
10	40452.34		

Table 3: Initial finite element analysis results compared with test results (mean values).

3.3 Property Identification

Using the mean measured values as target frequencies, input parameters of the FE model are updated by running an iterative, Bayesian estimation method [5].

The frequency difference between initial estimates and test values for the bending and torsional properties shows that a single updating parameter is not sufficient. Updating the Young's modulus will scale both frequencies to obtain a best trade off but will result in an overestimated bending frequency and underestimated torsional frequency (table 4). The relative difference with test data is shown between brackets.

Therefore, a second parameter must be introduced that affects one of the two modes in a different way. Considering the uncertainty on the torsional moment of inertia, this property is included as an additional updating parameter (table 5). The scatter plot in figure 3 also indicates that more than one random parameter should be used.

	Before Updating	After Updating
Young's Modulus	60 GPa	71.37 GPa
Bending	5268.82 Hz (-4.83%)	5746.66 Hz (3.80%)
Torsion	17594.87 Hz (-11.56%)	19190.59 Hz (-3.54%)

Table 4: Model updating using Young's modulus as parameter.

	Before Updating	After Updating
Young's Modulus	60 GPa	66.24 GPa (+10%)
Torsional Moment	2.36E-10 mm ⁴	2.73E-10 mm ⁴ (+16)
Bending	5268.82 Hz (-4.83 %)	5536.21 Hz (0 %)
Torsion	17594.87 Hz (-11.56 %)	19894.50 Hz (0 %)

Table 5: Model updating using Young's modulus and Ix torsional moment of inertia as parameters.

The results in table 5 show that complete convergence is obtained when E and Ix are both used as updating parameters. The resulting Young's modulus is in line with handbook values for aluminum and is 10% higher than the starting value. The torsional moment has to be increased by almost 16% compared to the starting value.

3.4 Probabilistic Analysis

The next step is to randomize these properties and simulate the scatter on the output responses as a result of applying a probability distribution. A normal distribution is assumed for both E and Ix. Their mean values are the values obtained after updating. The standard deviation can be estimated from the experimental scatter and the sensitivity of the bending and torsional frequencies for a perturbation of E and Ix using a probabilistic method.

A method that is applicable for this type of analysis is the Mean Value method (MV). From the Taylor series expansion that relates responses and parameters, truncated to the linear term, the following expression for standard deviation $\sigma_{R_j}^2$ of the responses can be obtained:

$$\sigma_{R_j}^2 \approx \sum_{i=1}^n S_{j,i}^2 \sigma_{P_i}^2 \quad (2)$$

With $S_{j,i}^2$ the first-order gradients (= sensitivities) and $\sigma_{P_i}^2$ the standard deviation of the parameters (~scatter). The sensitivities are readily available through finite element analysis [5] and $\sigma_{R_j}^2$ are known from statistical analysis of the test data (table 2) so that this equation 2 can be solved for the unknown $\sigma_{P_i}^2$.

The resulting random properties for E and Ix are shown in table 6.

	Mean value	Scatter (%)	PDF Type
Young's Modulus	66.24 GPa	0.0972	Normal
Torsional Moment	2.73E-10 mm ⁴	0.3029	Normal

Table 6: Random properties for Young's modulus and torsional moment of inertia.

The random parameter properties are used to generate 100 random Monte Carlo samples and re-analyze the FE model with the sample values. The resulting 100 bending and torsional frequencies are statistically postprocessed. The results are shown in table 7.

Mode	Mean (Hz)	St Dev (Hz)	Min (Hz)	Max (Hz)	Scatter (%)
Bending	5.5363E+3	2.6288E+0	5.5300E+3	5.5418E+3	0.04748
Torsion	1.9899E+4	3.1308E+1	1.9824E+4	1.9983E+4	0.1573

Table 7: Random properties of the responses.

The values for scatter in the last column of table 7 correspond very well with the experimental values (table 2).

In figure 6 the scatter plot resulting from the Monte Carlo sampling is overlaid with the reference test data cloud. It shows that the position, orientation, shape and size ("POSS") of the two point clouds match sufficiently well and no further iterations are required.

Note that, given the shape of the histograms in figures 4 and 5, the assumption of a normal distribution for the random parameters can be questioned. Using another distribution type that produces a sharper PDF should be more appropriate and further improve point cloud correlation.

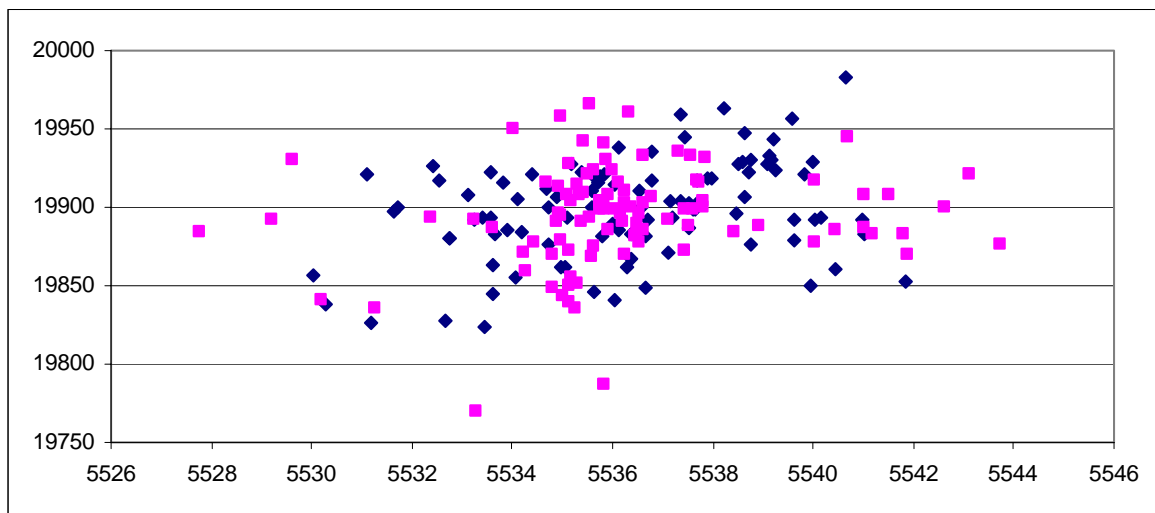


Figure 6: Overlaid scatter plots of test (dark) and simulation (light) resonance frequencies.

As was demonstrated before, at least two random parameters are required to obtain this result. To confirm that randomizing only the Young's modulus E is not sufficient, the overlaid scatter plots for this case is shown in figure 7. Although position and size are matching, the shape correlation of the two point clouds is not satisfactory and so this simulation does not sufficiently represent reality.

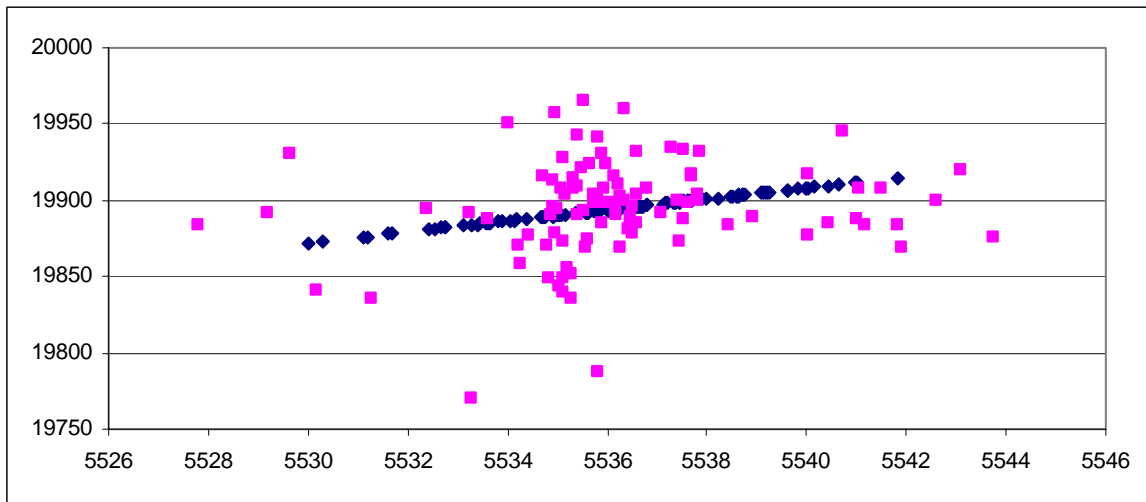


Figure 7: Overlaid scatter plots of test (dark) and simulation (light) resonance frequencies in case only the E-modulus is randomized.

3.5 Numerical Uncertainty in FE Analysis

To investigate spreading on the finite element analysis results, two FE models were made, one with 2736 Hex8 elements (using 6 X 6 element grid to model a section) and one with 3D general beam elements using increasing element density between 5 and 200 elements. In addition, the analysis was repeated with lumped and consistent mass distribution, and using different standard analysis codes (NASTRAN, ANSYS, ABAQUS). In total, 18 different analysis cases were solved. The material properties were set to Young's modulus of 60 GPa, mass density of 2703 kg/m³ and Poisson ratio of 0.3.

Figure 8 shows the results for the 7 first resonant frequencies using beam elements with lumped mass for increasing element density. The 5th frequency is the torsional mode; the other frequencies are bending modes that appear in pairs (in-plane, out of plane). It was concluded that minimum 20 elements are required. The analysis using consistent mass was less sensitive to mesh density. There was almost no difference between the analysis codes.

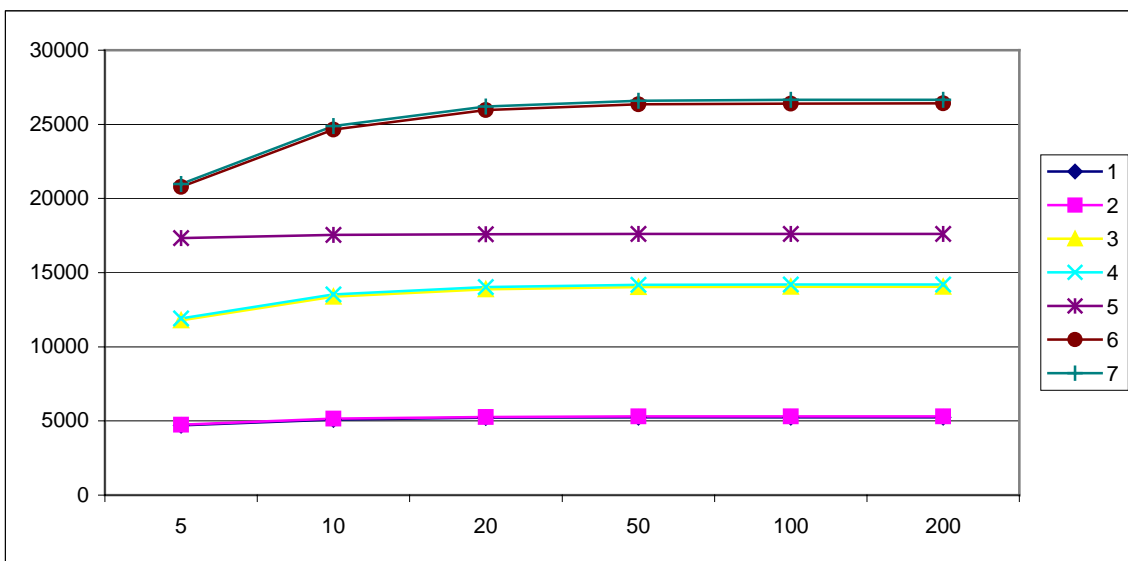


Figure 8: Resonance frequencies as function of the mesh density (beam elements with lumped mass).

The analysis results obtained using Hex8 elements also showed large consistency between the analysis codes with differences only due to the mass distribution.

The results could be reduced to 10 different sets of unique combinations of bending and torsional resonant frequencies. The statistical information on these results is shown in table 8.

Mode	Mean (Hz)	St Dev (Hz)	Min (Hz)	Max (Hz)	Scatter (%)
Bending	5.283E+3	30.64	5.236E+3	5.309E+3	0.5799
Torsion	1.758E+4	132.60	1.735E+4	1.782E+4	0.7542

Table 8: Statistical properties of FE data (10 cases).

The scatter on the bending and torsional resonant frequencies is of same magnitude. This scatter, only due to numerical uncertainty in the simulation, is about ten times larger than the physical scatter on the test data of the bending resonant frequency (see table 2). Note that this conclusion applies to this example but should not be generalized. In practical situations that involve test data acquired under less favorable conditions, scatter on the test data may well surpass the scatter attributed to numerical uncertainty.

Figure 9 shows an overlaid scatter plot between the 10 retained solutions and the test data. The solution that was used in the previous sections 3.2 to 3.4 is circled. The procedure that was followed here was to select that one representative solution, update the simulation model so that the result coincides with the mean of the test point cloud, and then randomize the simulation model. The scatter on test data, which reflects the total physical and numerical uncertainty on the test data, is thus used to identify physical scatter on the random parameters. As can be seen from figure 9, numerical uncertainty on the finite element analysis results can be significant and should also be taken into account to further define the bounds of validity of the obtained identification results.

The numerical uncertainty is not stochastic but reflects the existence of a variety of acceptable starting models and analysis settings from which an engineer may choose depending on experience and judgment. It seems therefore appropriate to treat this type of numerical uncertainty using an interval method. However, such analysis was beyond the scope of the present paper.

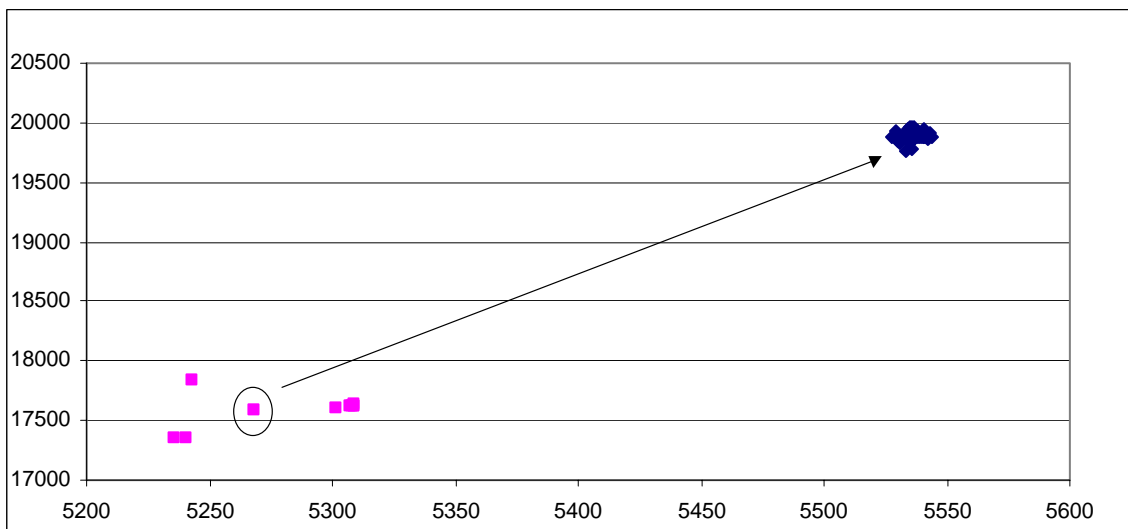


Figure 9: Overlaid resonance frequencies scatter plots of test (dark) and 10 different simulation cases (light).

4 Conclusions

A practical methodology was described to estimate the random properties of input parameters for finite element analysis using from scatter on reference test data, obtained from repeated testing. The method uses a combination of classical sensitivity-based model updating and probabilistic analysis in a two-step approach. A real-life example of identifying the material Young's modulus and beam section moment of inertia was used to demonstrate the procedure.

In addition to accounting for physical scatter on the input parameters, analysts should be aware of the numerical uncertainty that is inherent in every simulation. Future work should focus on how to incorporate numerical uncertainty in the procedure. Furthermore comparison or combining the results with other methods like the interval method [7] should be investigated.

Acknowledgements

The experimental data used in this paper was acquired and supplied in the framework of the GRAMATIC research project supported by the Flemish Institute for the Promotion of Scientific and Technological Research in Industry.

References

- [1] Dascotte E., *Material Identification of Composite Structures from the Combined Use of Finite Element Analysis and Experimental Modal Analysis*, Proceedings of the 10th International Modal Analysis Conference, February 1992, San Diego, California.
- [2] Lauwagie T., Dascotte E., *Layered Material Identification using Multi-Model Updating*. Proceedings of the 3rd International Conference on Structural Dynamics Modeling - Test, Analysis, Correlation and Validation - Madeira Island, Portugal, June 2002.
- [3] Dascotte E., *The Use of FE Model Updating and Probabilistic Analysis for Dealing with Uncertainty in Structural Dynamics Simulation*, Proceedings of the 2003 Japan Modal Analysis Conference (JMAC), September 10-12, 2003, Tokyo, Japan.
- [4] Marczyk J., *Statistical Validation of FE Models Using Experimental Data*, Proceedings of the 21st ISMA Conference. 1996.
- [5] FEMtools 3.0, Software for Correlation, Validation and Updating of FE Models, Dynamic Design Solutions N.V. www.femtools.com.
- [6] Lauwagie T., *The Spreading on the Resonance Frequencies of an Aluminum Beam*, KUL-PMA Internal Report, April 2004.
- [7] Lauwagie T., *Error Estimation in Material Identification*, KUL-PMA Internal Report, May 2003.